J Electroceram (2006) 17:241–245
DOI 10.1007/s10832-006-8315-8

Improvement of the thermal and chemical stability of Al doped ZnO films

I. H. Kim · D. Y. Ku · J. H. Ko · D. Kim · K. S. Lee · J.-h. Jeong · T. S. Lee · B. Cheong · Y.-J. Baik · W. M. Kim

Received: 27 June 2005 / Revised: 15 February 2006 / Accepted: 16 March 2006

Abstract To improve the stability of sputter-deposited ZnO:Al (AZO) films at high temperature above 300°C, an amorphous Zn-Sn-O (ZTO) film was deposited on the top of AZO films as an protective layer by co-sputtering of pure ZnO and SnO_2 targets. Amorphous ZTO films had resistivity in the range from 10^{-2} to 10^{-3} Ωcm and were stable up to temperature of 400°C. Heat treatments of bare AZO films in the atmosphere at 400°C resulted in a dramatic increase in the resistivity accompanied by substantial decrease in carrier concentration and Hall mobility. The AZO films covered with the ZTO film showed remarkable improvement in thermal stability for subsequent heat treatments in the temperature range from 200 to 400°C in the atmosphere as well as chemical stability in weak acidic solution. X-ray photoelectron spectroscopy analysis showed that the improvement was attained by ZTO layer acting as diffusion barrier of oxygens and/or water vapors.

Keywords Transparent conducting oxide · ZnO · Amorphous · Zinc stannate · ZTO · Thermal · Chemical · Stability

I. H. Kim (✉) · D. Y. Ku · K. S. Lee · J.-h. Jeong · T. S. Lee
B. Cheong · Y.-J. Baik · W. M. Kim
Thin Film Materials Research Center, Korea Institute of Science and Technology, 39-1, Hawolgok-dong, Sungbuk-gu, Seoul 136-791, Korea
e-mail: inhok@kist.re.kr

J. H. Ko · D. Kim
Division of Materials Science and Engineering, Korea University Anam-Dong 5-1, Sungbuk-gu, Seoul 136-701, Korea

1 Introduction

Transparent conducting oxide (TCO) films are oxide materials which are highly transparent to visible light and electrically conducting. TCO films, especially indium tin oxides (ITO, Sn doped In_2O_3) have been widely used in many applications such as transparent electrodes of flat panel devices, solar cells and IR reflectors [1]. Recently doped ZnO films with Al, Ga or In have attracted much attention as an alternative material of ITO due to their good advantages of the low electrical resistivity similar to ITO and the low material cost [2, 3]. However, practical applications of ZnO films have been limited because they are unstable at elevated temperatures above 300°C in the atmosphere and also easily etched in the weak acidic and basic solution [4, 5]. Their instability is attributed to the high chemical reactivity of ZnO materials. Minami has reported that new transparent and conducting oxides of amorphous zinc-stannate ($ZnSnO_3$) films are stable in an oxidizing environment at 300°C and also chemically stable in HCl and NaOH solutions and low resitive zinc-stannate films of 10^{-2}–10^{-3} Ωcm can be obtained at room temperature [6, 7].

Due to chemical and thermal stability of the zinc-stannate (ZTO) films, these films may be used as a protective layer for ZnO based TCO films such as Al doped ZnO (AZO) films whose practical applicability is limited by thermal or chemical instability. In this article, ZTO-coated ZnO films were prepared by radio frequency (rf) magnetron sputtering, and their thermal and chemical stabilities were investigated.

2 Experimental details

Al doped ZnO films were deposited on glass substrates (Corning Eagle 2000) by rf magnetron sputtering from a

2-inch diameter target composed of ZnO and Al_2O_3 2 wt%. The base pressure in the chamber was below 6.7×10^{-5} Pa. Sputtering deposition was carried out under a working pressure of 0.133 Pa in pure Ar gas at a power of 50 W. During the deposition of AZO films, substrate temperature was kept at 150°C. After deposition of AZO film with thickness of 300 nm, the substrate was cooled to room temperature, and the deposition of ZTO top layer was followed on top of AZO film in situ without intentional heating of the substrate. ZTO top layer was deposited by co-sputtering of pure ZnO and SnO_2 targets in 1.25% O_2 mixed with Ar gas. To examine the dependence of ZTO top layer thickness, ZTO top layers with two different thicknesses of 30 and 100 nm were deposited. The rf powers on ZnO and SnO_2 targets were 20 and 42 W, respectively. The Zn content in present ZTO film, Zn/(Zn + Sn) ratio, determined from EPMA was 0.27. It is known that zinc stannate near this composition has low resistivity of 10^{-3} Ωcm and its resistance is thermally stable in air [6]. In the following analysis, the sample identifications of AZO/ZTO30 and AZO/ZTO100 will be used to designate the AZO film with ZTO top layer of thickness 30 and 100 nm, respectively. A ZTO film of 300 nm thickness was also prepared to examine their electrical end optical properties. To examine the thermal stability, AZO and ZTO coated AZO films were heat treated at temperatures of 200 to 400°C in air for one hour.

The electrical resistivity, Hall mobility and carrier concentration were determined from a Hall measurement equipment using a Van der Pauw method. For study of chemical stability, resistance changes were measured with AZO and ZTO coated AZO films immersed in the 0.1 M HCl solution as functions of elapsed time. For analysis of oxygen compositions and the binding energy of oxygens, depth profiles of X-ray photoelectron spectroscopy (XPS) were obtained for the as-deposited and the heat-treated films. Film structure was analyzed using X-ray diffractometer (Rigaku). The composition of ZTO film, i.e. Zn and Sn contents, was determined by electron probe micro analysis (EPMA). Using atomic force microscopy (AFM, Digital Instrument), the surface morphologies of AZO, ZTO and ZTO coated AZO films were analyzed. The optical transmission spectra were obtained using UV-visible spectrophotometer (Perkin Ellmer) in the wavelength range from 250 to 1100 nm.

3 Results and discussions

The variations in resistivity, Hall mobility and carrier concentration of AZO and ZTO films as a function of heat treatment temperature are shown in Fig. 1(a) and (b). The XRD pattern of as-deposited ZTO film exhibited only broad peak at 2θ–34° characteristic of amorphous zinc tin oxide

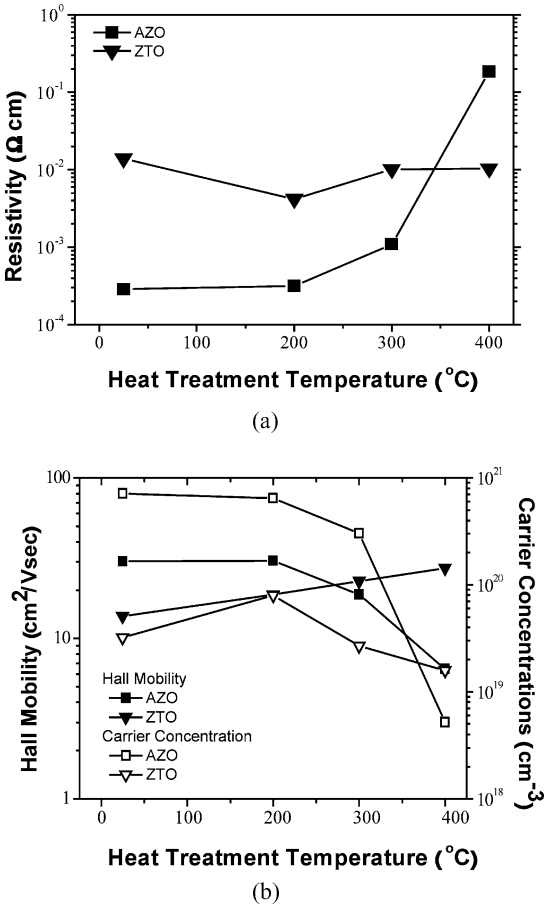

Fig. 1 (a) Electrical resistivity, (b) Hall mobility and carrier concentration of AZO and ZTO films as a function of heat treatment temperature

films reported in the literature [8, 9]. The resistivity of the as-deposited AZO film was 2.9×10^{-4} Ωcm. The AZO film was relatively stable up to heat treatment temperature of 200°C. At the heat treatment temperature of 300°C, the resistivity of AZO film increased moderately, reaching 1.1×10^{-3} Ωcm. But for heat treated AZO film at temperature of 400°C, the resistivity increased almost three orders of magnitude, amounting to as high as 0.18 Ωcm. This large change in resistivity is mainly attributed to the decrease of carrier concentrations because carrier concentrations changed by over two orders of magnitude from 7.2×10^{20} to 5.2×10^{18} cm^{-3}, while the Hall mobility decreased moderately from 30.3 to 6.5 cm^2/Vsec. Unlike the AZO films, the resistivity of ZTO films decreased slightly upon heat treatment, showing the minimum resistivity value of 4.16×10^{-3} Ωcm at temperature of 200°C. Hall measurement showed that the decrease in the resistivity of ZTO films was resulted from the increase of Hall mobility, which might be caused by the enhancement of structural orderness of amorphous ZTO films through annealing. The carrier concentration showed the maximum value at 200°C, and decreased slightly at higher temperatures. The carrier concentration of the heat treated

ZTO film at 400°C was 1.6×10^{19} cm^{-3}, one half of that of as-prepared film, indicating that ZTO films are very stable even in an oxidizing environment because oxygen vacancies are thought to be the major source of free carriers in ZTO films [9]. The XRD measurement revealed that the ZTO film maintained its amorphous structure even after the heat treatment at 400°C. This structural stability at high temperature might help a lot for ZTO films to be stable in the electrical properties.

In Fig. 2(a) and (b), the changes in electrical resistivity and the corresponding changes in Hall mobility and carrier concentration of ZTO coated AZO films are plotted as a function of heat treatment temperatures, respectively. The changes in electrical resistivity of bare AZO film shown in Fig. 1(a) are also plotted in Fig. 2(a) for comparison's sake. The resistivities of the as-prepared AZO/ZTO30 and AZO/ZTO100 samples were 3.2×10^{-4} and 3.7×10^{-4} Ωcm, respectively. The heat treatment at the temperature of 300°C did not cause any noticeable change in resistivities of both AZO/ZTO30 and AZO/ZTO100 samples. The heat treatment at the temperature of 400°C resulted in the increase of the resistivities. But the resistivities of AZO/ZTO30 and AZO/ZTO100 samples were 4.8×10^{-3} Ωcm and 1.0×10^{-3} Ωcm respectively, which were more than one to two orders of magnitude lower than that of bare AZO film treated at the same temperature. The exactly same trends in Hall mobility and carrier concentration of ZTO coated AZO samples as the electrical resistivity are reflected in Fig. 2(b). The experimental values of resistivity, carrier concentration and Hall mobility of as-prepared ZTO coated AZO samples were comparable to those calculated using a simple model applied for the case of resistors connected in parallel [10].

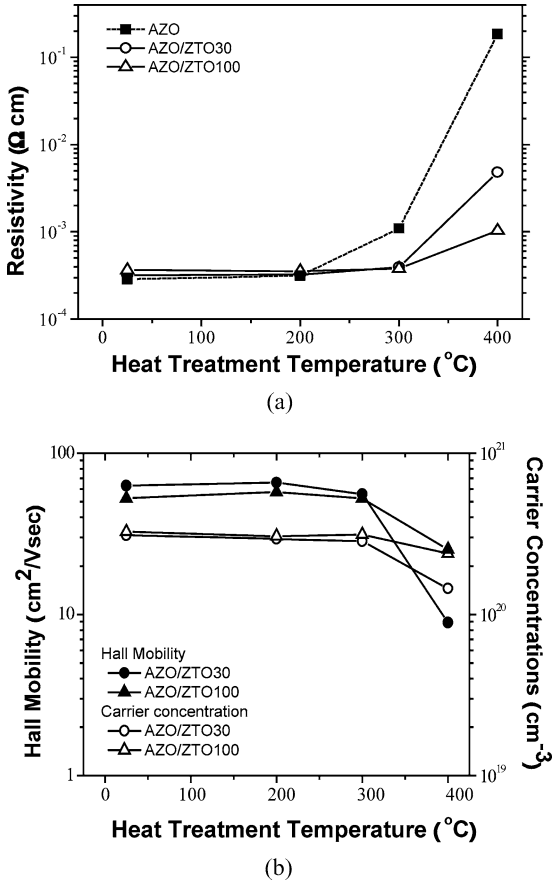

Fig. 2 (a) Electrical resistivity, (b) Hall mobility and carrier concentration of ZTO coated AZO films with ZTO thickness of 30 and 100 nm as a function of heat treatment temperature

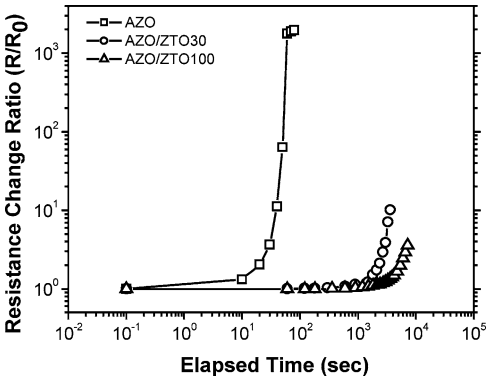

Fig. 3 Ratio of resistance change in bare AZO and ZTO coated films in HCl 0.1 M as a function of elapsed time (R_0 = initial resistance)

Chemical stability of bare AZO film and ZTO coated AZO films were analyzed by immersing them in a weak acidic solution of 0.1 M HCl. The samples were electrically connected to a multi-tester by Au wires, and their resistance changes were monitored with elapsed time in solution. Figure 3 shows the electrical resistance changes of bare AZO film and ZTO coated AZO films in 0.1 M HCl solution. The bare AZO film was completely etched away after only about 50 s. But the significant increases in the resistances (factor of 2) were observed only after 40 min and 90 min for AZO/ZTO30 and AZO/ZTO100 sample respectively. The improved chemical stability of ZTO coated AZO films is due to Sn element in ZTO top layer which is chemically inactive [11].

AZO is a *n*-type semiconductor where the free carriers are generated by the substitution of Al for Zn and interstitial Zn atoms. The dramatic increase of the resistivity of AZO films above 300°C has been explained by the chemisorption of oxgyens at film surfaces and grain boundaries of the film and an oxidation of interstitial Zn atoms [4]. The chemisorbed oxygens act as trap sites of free carriers, reducing the free carriers in grains of ZnO films. And the trapped carriers cause increase of grain boundary potential barriers, leading to reduction of the Hall mobility of ZnO films [12]. To clarify the role of ZTO layer as diffusion barrier of oxygens or water vapors, oxygen binding energy analysis using XPS was carried

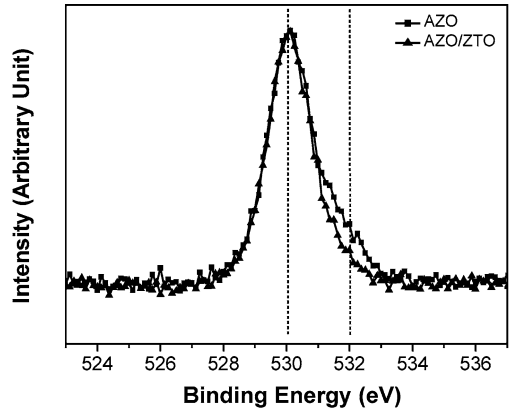

(a)

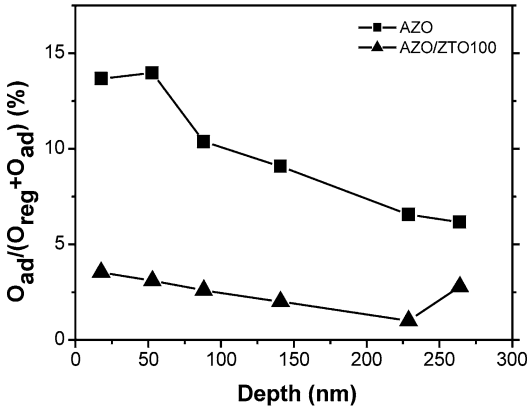

(b)

Fig. 4 (a) XPS spectra of O 1s of bare AZO film and the ZTO coated AZO film with ZTO thickness of 100 nm. The spectra was obtained at the AZO film position of about 18 nm deep from the surface for bare AZO film and from the ZTO interface for ZTO coated AZO sample. (b) Variation of the ratio $O_{ad}/(O_{ad} + O_{reg})$ inside AZO layer with depth for bare AZO film and ZTO coated AZO film

out. Figure 4(a) shows O 1s XPS spectra of bare AZO film and AZO/ZTO100 sample obtained after sputter etching of about 18 nm thick AZO layer from the air interface or from the ZTO interface, respectively. The O 1s spectra of bare AZO film clearly shows shoulder at high binding energy side, and can be deconvoluted into two peaks. Main peak is located about 530.0 eV and a smaller peak is located at 532.0 eV. The main peak at 530.0 eV is attributed to O-Zn bonds, while the peak at 532.0 eV stemming from-OH bonds, chemisorbed O_2^- and O^- at grain boundaries [13]. The O 1s spectra obtained from the AZO layer of the AZO/ZTO100 sample shows much smaller shoulder at 532.0 eV than that of bare AZO film. Since ZTO layer was deposited on top of the AZO film in situ, it is deduced that the large shoulder peak of bare AZO film is caused by the chemisorption followed by the diffusion of oxygens and water vapors along grain boundaries which are the high diffusivity paths [14], once the film is exposed to atmosphere. Because amorphous ZTO top layer has no

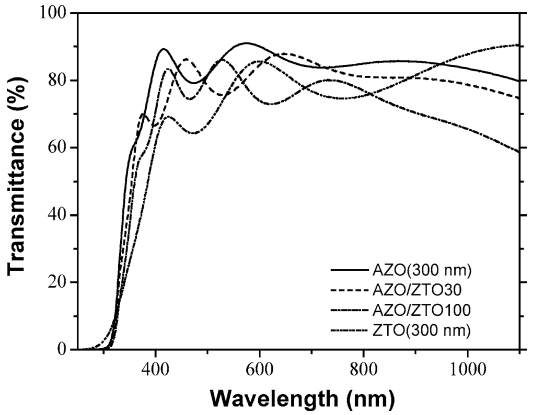

Fig. 5 Transmittance spectra of bare AZO film, ZTO film and ZTO coated AZO films in the wavelength range from 250 to 1100 nm

grain boundaries, the diffusion of chemisorbed oxygens and water vapors into the AZO layer will be hindered substantially, resulting in much smaller shoulder peak at 532.0 eV. Figure 4(b) shows the results of XPS depth profiling of the corresponding samples, expressed in the form of the ratio $O_{ad}/(O_{ad} + O_{reg})$ where O_{ad} represents content of oxygen bonds from -OH bonds, chemisorbed O_2^- and O^- at grain boundaries and O_{reg} represents content of oxygens bonded to Zn. For both samples, O_{ad} showed dependence on depth, showing a decreasing trend with depth. Furthermore, the ratio $O_{ad}/(O_{ad} + O_{reg})$ in bare AZO film at the near surface was amounting to 14%, while that in AZO layer of the AZO/ZTO100 sample at near interface being only 4%. The above XPS results clearly shows that the degradation of ZnO films is caused by chemisorption and diffusion of oxygens and/or water vapors, and that amorphous ZTO layer can be used to prevent or to retard the degradation of doped ZnO films.

In Fig. 5, transmittance spectra of AZO/ZTO30 and AZO/ZTO100 samples are compared with those of AZO and ZTO monolayer of 300 nm thickness. Average transmittances in the visible range were 75, 78, 82 and 86% for ZTO monolayer, AZO/ZTO30, AZO/ZTO100 and bare AZO film, respectively. The low optical transmission of ZTO film in visible region, especially in short wavelength region, stems partly from the absorption due to finite value of extinction coefficient and partly from the high refractive index value of ZTO (2.06 at 530 nm) compared to that of IZO(1.84 at 530 nm). The transmission loss can be minimized by reducing the extinction coefficient of ZTO film and also by designing layer thickness such as use of half wavelength thickness. The root-mean squared (rms) surface roughness of bare AZO film was 1.8 nm, and that of the ZTO film was only 0.3 nm. The morphology of ZTO coated AZO films were very similar to bare AZO film, giving rms surface roughness values of about 2.0 and 1.6 nm for AZO/ZTO30 and AZO/ZTO100 sample respectively.

4 Conclusions

The AZO films showed the significant increase of the resistivity above the temperature of 300°C and the chemical instability in the weak acidic solution. For the improvement of thermal and chemical stabilities of AZO films, the amorphous ZTO films were coated on the top of AZO films in situ at room temperature. The increase in electrical resistivity for the ZTO coated AZO films upon heat treatment in the atmosphere was substantially reduced, and the chemical stability in weak HCl solution was also greatly improved. From the XPS analysis, it was confirmed that the amorphous ZTO films were acting as a diffusion barrier for the chemisorbed oxygens and/or water vapors in the atmosphere, leading to improved thermal stability. Since amorphous ZTO films can provide appropriate electrical resistivity and optical transparency as well as good surface morphology, doped ZnO films coated with amorphous ZTO layer can be applied for the practical TCO applications where doped ZnO films can not sustain the required properties.

References

1. D.S. Ginley and C. Bright, *MRS Bull.*, **25**(8), 15 (2000).
2. K. Ellmer, *J. Phys. D: Appl. Phys.*, **34**, 3097 (2001).
3. T. Minami, *MRS Bull.*, **25**(8), 38 (2000).
4. T. Minami, H. Nanto, S. SHooji, and S. Takata, *Thin Solid Films*, **111**, 167 (1984).
5. A. Valentini, F. Quaranta, M. Penza, and F.R. Rizzi, *J. Appl. Phys.*, **73**(3), 1143 (1992).
6. T. Minami, H. Sonohara, S. Takata, and H. Sato, *Jpn. J. Appl. Phys.*, **33**, L1693 (1994).
7. T. Minami, S. Takata, H. Sato, and H. Sonohara, *J. Vac. Sci. Technol. A*, **13**(3), 1095 (1995).
8. T. Moriga, Y. Hayashi, K. Kondo, Y. Nishimura, K. Murai, and I. Nakabayashi, *J. Vac. Sci. Technol.*, **A 22**(4), 1705 (2004).
9. Y. Hayashi, K. Kondo, K. Murai, T. Moriga, I. Nakabayashi, H. Fukumoto, and K. Tominaga, *Vacuum*, **74**, 607 (2004).
10. K. Tominaga, N. Umezu, I. Mori, T. Ushiro, T. Moriga, and I. Nakabayashi, *Thin Solid Films*, **334**, 35 (1998).
11. R.G. Gordon, *MRS Bull.*, **25**(8), 52 (2000).
12. S. Ghosh, A. Sarkar, S. Chaudhuri, and A.K. Pal, *Thin Solid Films*, **205**, 64 (1991).
13. M.K. Puchert, P.Y. Timbrell, and R.N. Lamb, *J. Vac. Sci. Technol.*, A **14**(4), 2220 (1996).
14. H. Geistlinger, *J. Appl. Phys.*, **80**(3), 1370 (1996).